ARTICLE

σ or π? Bonding interactions in a series of rhenium metallotetrylenes

Received 00th January 20xx,
Accepted 00th January 20xx

DOI: 10.1039/x0xx00000x

Erik T. Ouellette,[ab] Ambre Carpentier,[c] I. Joseph Brackbill,[ab] Trevor D. Lohrey,[ab] Iskander Douair,[c] Laurent Maron,[c] Robert G. Bergman,[a] John Arnold*[ab]

Salt metathesis reactions between a low-valent rhenium(I) complex, Na[Re(η^5-Cp)(BDI)] (BDI = N,N′-bis(2,6-diisopropylphenyl)-3,5-dimethyl-β-diketiminate), and a series of amidinate-supported tetrylenes of the form ECl[PhC(N^{t}Bu)$_2$] (E = Si, Ge, Sn) led to rhenium metallotetrylenes Re(E[PhC(N^{t}Bu)$_2$])(η^5-Cp)(BDI) (E = Si (**1a**), Ge (**2**), Sn (**4**)) with varying extents of Re–E multiple bonding. Whereas the rhenium-stannylene **4** adopts a σ-metallotetrylene arrangement featuring a Re–E single bond, the rhenium-silylene (**1a**) and -germylene (**2**) both engage in additional π-interactions to form short Re–E multiple bonds. Temperature was found to play a crucial role in reactions between Na[Re(η^5-Cp)(BDI)] and SiCl[PhC(N^{t}Bu)$_2$], as manipulation of reaction conditions led to isolation of an unusual rhenium-silane, (BDI)Re(μ-η^5:η^1-C_5H_4)(SiH[PhC(N^{t}Bu)$_2$]) (**1b**) and a dinitrogen bridged rhenium-silylene, (η^5-Cp)(BDI)Re(μ-N_2)Si[PhC(N^{t}Bu)$_2$] (**1c**), in addition to **1a**. Finally, the reaction of Na[Re(η^5-Cp)(BDI)] with $GeCl_2$·dioxane led to a rare μ_2-tetrelido complex, μ_2-Ge[Re(η^5-Cp)(BDI)]$_2$ (**3**). Bonding interactions within these complexes are discussed through the lens of various spectroscopic, structural, and computational investigations.

Introduction

The thoughtful design of transition metal–main group multiply-bonded systems has the potential to facilitate cooperative activations of small molecules and other catalytically relevant transformations.[1] Multiple bonds between carbon and transition metals have been studied extensively, and many such systems play integral roles in organic synthesis and industrial catalysis.[2–9] By studying the orbital interactions within these metal-carbon multiple bonds, including the factors that lead to Fischer- (electrophilic at carbon) versus Schrock- (nucleophilic at carbon) type carbenes and carbynes, researchers have been able to prepare complexes with desired modes of reactivity.

In contrast to metal-carbon multiple bonds, the breadth of molecular chemistry possible with heavier group 14 elements (*e.g.* Si, Ge, Sn) has yet to be fully realized. In comparison to carbon, these elements have large energy gaps between their *s* and *p* orbitals which disfavors *s-p* mixing.[10,11] Accordingly, the study of the heavier analogues of transition metal carbenes and carbynes, known as tetrylenes or tetrylynes, could lead to the characterization of electronic properties and modes of reactivity substantially different from those of their carbon-containing relatives.

Investigations have already led to the synthesis of a variety of transition metal tetrylenes[1,12–23] and tetrylynes,[24–28] most of which act as Fischer-type complexes.[24] Two main synthetic pathways to transition metal-heavy group 14 multiple bonds incorporate divalent tetrylene precursors (Figure 1a): (1) salt metathesis of a halotetrylene with an anionic metal species to form a σ-metallotetrylene, followed by ligand dissociation at the metal (in this case to form the first reported metal

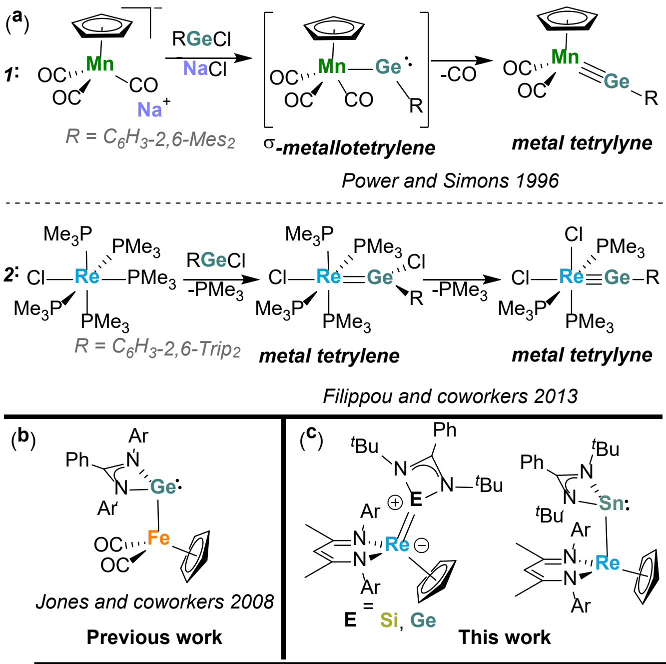

Figure 1. (**a**) Two pathways to transition metal-heavy group 14 multiple bonding: (1) salt metathesis to form a σ-metallotetrylene, followed by ligand dissociation to form a metal-tetrylyne,[26] and (2) tetrylene ligand substitution to form a metal tetrylene, followed by halide migration to form a metal tetrylyne. (**b**) Structure of the only previously reported amidinate-supported σ-metallotetrylene.[33] (**c**) Structures of the rhenium-tetrylene complexes reported herein.

[a] Department of Chemistry, University of California, Berkeley, California, 94720, USA.
[b] Chemical Sciences Division, Lawrence Berkeley National Laboratory, Berkeley, California, 94720, USA. E-mail: arnold@berkeley.edu.
[c] LPCNO, Université de Toulouse, INAS Toulouse, 135 Avenue de Rangueil, 31077, Toulouse, France.

†Electronic Supplementary Information (ESI) available: Synthetic procedures and characterization information (PDF) and corresponding CIF files (CIF). CCDC 2048928–2048933. See DOI: 10.1039/x0xx00000x

tetrylyne),[26] and (2) dative ligand substitution/association at the metal by a tetrylene to form a metal tetrylene, which in certain cases undergoes halide migration to form a metal tetrylyne (these complexes represent the first reported examples of rhenium germylenes and germylynes).[29] For typical halotetrylene precursors (ERX or EX_2), these pathways are relatively straightforward, however we became interested in the use of a newer class of amidinate-supported halotetrylenes to form metal-heavy group 14 multiple bonds.[30–32] While such tetrylenes have been found to bind to a vast number of metal centers through donation of the tetrylene-centered lone pair,[13,19,22] there is only one reported example of salt metathesis between an amidinate-supported tetrylene and a transition metal species; reaction of a η5-cyclopentadienyl dicarbonyl iron (Fp) salt with an amidinate-supported germylene resulted in an iron σ-metallotetrylene complex devoid of multiple bonding interactions (Figure 1b).[33] Considering a highly nucleophilic rhenium(I) salt synthesized by our group has been shown to behave as a strong π-donor and participate in reactivity unseen in analogous Fp systems,[34] we hypothesized that the use of such a metal complex might compel the formation of π-bonding interactions with amidinate-supported tetrylene reagents. Employing a π-donor strategy to form M–E multiple bonds should lead to novel amidinate-supported complexes, and the resulting increase in relative electron density at the group 14 atom may allow for a shift in reactivity from more traditional Fischer-type tetrylenes and tetrylynes.

Here we report reactions of Na[Re(η^5-Cp)(BDI)] (BDI = N,N'-bis(2,6-diisopropylphenyl)-3,5-dimethyl-β-diketiminate),[35] with the chlorotetrylenes ECl[PhC(N*t*Bu)$_2$] (E = Si, Ge, Sn), along with $GeCl_2$·dioxane, $SnCl_2$, and $PbCl_2$ (for an amidinate-free comparison), and our examinations of the unusual bonding motifs present in the subsequent product complexes, achieved through a variety of spectroscopic, structural, and computational investigations (Figure 1c).

Results and Discussion

Mixing of the chlorosilylene, SiCl[PhC(N*t*Bu)$_2$], with Na[Re(η^5-Cp)(BDI)] in THF at ambient temperature for one hour led to the formation of two isomeric products that could be separated on the basis of their contrasting solubilities. Extraction of the crude reaction residue with pentane and subsequent crystallization enabled the isolation of a rhenium-silylene complex, Re(Si[PhC(N^{t}Bu)$_2$])(η^5-Cp)(BDI) (**1a**) in 37 % yield, whereas a rhenium-silane, (BDI)Re(μ-η^5:η^1-C_5H_4)(SiH[PhC(N^{t}Bu)$_2$]) (**1b**), was extracted and crystallized from Et_2O in 15 % yield (Scheme 1). Integrations from a ^{1}H NMR spectra of a crude mixture of **1a**/**1b** products prior to any separation suggested the formation of **1a** to **1b** in a 65:35 ratio. We suggest that complex **1b** is formed via migration of a hydrogen atom from the cyclopentadiene (Cp) ligand to the silicon center to give a bridging silane. The Si–*H* ^{1}H NMR resonance of bridging silane **1b** manifests as a doublet at 5.74 ppm, suggesting weak, long-range coupling with the Cp proton resonance found at 4.70 ppm, which is confirmed by a cross peak in the ^{1}H-^{1}H COSY spectrum (Figure S4). The silane proton resonance also displays satellite peaks enabling determination of the large ^{29}Si–^{1}H coupling constant ($^1J_{Si,H}$ = 238.1 Hz). A band at 2128 cm^{-1} in the infrared spectrum of **1b**, attributable to an Si–H stretch, further confirms our assignment of silane complex **1b** (Figure S27). A ^{29}Si{^{1}H} resonance was observed for **1b** at –58.3 ppm, which is shifted upfield relative to the chlorosilylene starting material (δ = 14.6 ppm)[30] and falls within an expected range for transition metal silyls.[36] Unfortunately, attempts to locate a ^{29}Si{^{1}H} NMR signal for silylene **1a** proved unsuccessful.

Interestingly, a reaction between these same starting materials in diethyl ether at –78 °C followed by a cold workup and crystallization from pentane allowed for the observation of a new dinitrogen-bridged silylene product, (η^5-Cp)(BDI)Re(μ-N_2)Si[PhC(N^{t}Bu)$_2$] (**1c**), which forms in a 75:25 ratio to minor product silylene **1a** based on ^{1}H NMR integrations of the crude product mixture. Despite multiple crystallization attempts, we were unable to isolate dinitrogen-bridged silylene **1c** as a pure, bulk material, but infrared absorbance measurements of the product mixture revealed an N–N stretch at 1682 cm^{-1}, indicating significant weakening of the N–N bond relative to free N_2 (ν_{NN} = 2359 cm^{-1})[37] (Figure S28). Formation of **1c**, in which a molecule of dinitrogen from the reaction atmosphere has been incorporated into the complex, is not entirely unexpected given recent results from our group indicating that Na[Re(η^5-Cp)(BDI)] reversibly binds N_2 in solution.[34,38] While we were able to observe dinitrogen-bridged silylene **1c** via ^{1}H and ^{29}Si{^{1}H} NMR, IR, and X-ray diffraction (see below), further characterization was hampered by the instability of **1c** at ambient temperature.

Solutions of dinitrogen-bridged silylene **1c** in benzene-d_6 left at ambient temperature were monitored by ^{1}H NMR, which showed slow conversion of **1c** to the bridging silane **1b** (Scheme 1, Figure S8). Our attempts to convert pure samples of silylene **1a** directly to **1b** – either at elevated or ambient temperature in solution – were unsuccessful, instead leading to decomposition

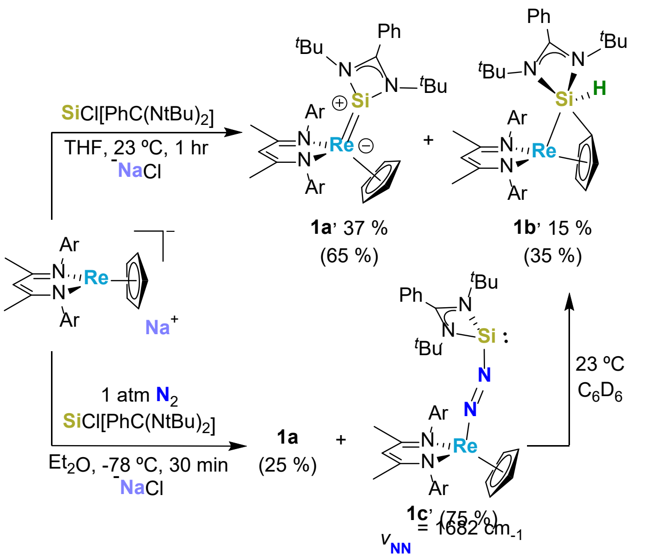

Scheme 1. Syntheses of complexes **1a-c**. Product ratios shown in parentheses are determined by ^{1}H NMR and isolated yields are shown without parentheses. Dinitrogen-bridged silylene **1c** decomposes to bridging silane **1b** in benzene-d_6 solution at ambient temperature over several days (no yield determined for this conversion).

Please do not adjust margins

of **1a**. It is likely that even at ambient temperature, the dinitrogen-bridged **1c** acts as a transient intermediate along the path to forming **1b**; since binding of dinitrogen by Na[Re(η^5-Cp)(BDI)] is lower at ambient temperature (compared to at –78 °C), **1c** is formed as a minor species relative to **1a** and rearranges to the minor product, **1b**. In contrast, binding of dinitrogen by Na[Re(η^5-Cp)(BDI)] is favored at –78 °C, leading to formation of the dinitrogen-bridged **1c** as a major product since the cold workup impedes decomposition to **1b**.

The solid-state structures of **1a-c** were determined by single crystal X-ray diffraction (Figure 2). Complex **1a** displays a short Re–Si bond of 2.2413(9) Å, which is the shortest Re–Si bond reported by 0.154(2) Å.[39] Additionally, Re1–Si1–N3/N4 angles of 138.90(9)° and 151.4(1)° (sum of bond angles about Si: 359.4°) illustrate a roughly trigonal planar geometry about the silicon center (see Figures S20-22 for additional perspectives of **1a-c**). This short, planar coordination of the amidinate-supported silylene to rhenium suggests the absence of a non-bonding silicon-centered lone pair (as is observed in the silylene starting material); these electrons are likely involved in bonding interactions with rhenium. The amidinate *tert*-butyl groups in silylene **1a** are distinguishable in the ^{1}H NMR spectrum, indicating lack of free rotation about the Re–Si bond in solution, which corroborates the hypothesis of multiple bonding interactions that lock this orientation in place.

In contrast, we find a Re1–Si1 bond distance of 2.5299(8) Å in bridging silane **1b**, consistent with a rhenium-silicon single bond. The silane hydrogen was located in the difference map and refined isotropically. While we have previously observed substitution at one of the Cp carbons in conjunction with migration of a Cp hydrogen to form a rhenium hydride,[34] this present result differs in that the hydrogen instead migrates to silicon, leading to an unusual bridged bonding arrangement in which silicon is bonded to five atoms. Despite the nonplanar bonding between silicon and a formally sp^2 Cp carbon (Si1–C1: 1.868 Å), the Cp ring remains bound to rhenium in an η^5 fashion (Re–C bond lengths: 2.182(2)-2.244(2) Å, C–C bond lengths 1.409(3)-1.453(3) Å). While there are reported examples of metallocenophanes featuring a silane bridge between two *trans* C_5H_4 ligands,[40] there are no structurally characterized complexes displaying a silane bridge between a C_5R_4 ligand and the metal center, as in **1b**. The Re–Si–N3/N4 angles in **1b** of 113.80(6)° and 140.38(6)° are smaller than those observed in **1a** and highlight deviations from the planar bonding arrangement of **1a**.

Dinitrogen-bridged silylene **1c** is different from **1a** and **1b** in that there is no direct rhenium-silicon contact, with the molecule instead containing a diazenide fragment with a N3–N4 bond distance of 1.19(2) Å, which is elongated relative to that of free N_2 (1.098 Å).[41] The N4–Si1–N5/N6 angles of 96.8(3)° and 98.0(4)° are relatively small and consistent with similar angles in the SiCl[PhC(N^{t}Bu)$_2$] starting material, indicating the silylene center in **1c** preserves a non-bonding lone pair orbital.

We were intrigued by the unusual structural metrics displayed within these molecules, so we next turned to density functional theory (DFT) using the B3PW91 functional (see ESI for complete computational details) and natural bond orbital (NBO) analyses for each compound. In silylene **1a**, we found two discrete bonding interactions that can be described through the use of qualitative frontier orbitals for the rhenium (as derived from a qualitative molecular orbital analysis of M(η^5-Cp)(L)$_2$ fragments, Figure 3a)[42] and silicon (Figure 3b) fragments. The first interaction is of σ-symmetry and is formed by overlap of an s/p_z-hybdridized silicon lone pair with the rhenium *3a′* orbital (Figure 3c, percent NBO contributions can be found in Table S5). A second bonding interaction, one of π-symmetry, is made up by overlap of rhenium *a″* and silicon p_x orbitals. Additionally, second-order perturbation analysis revealed one of the remaining filled *d*-orbitals on rhenium, referred to as the a_π' orbital in this case, to be delocalized towards a silicon p_y orbital in a donation interaction of roughly 60 kcal/mol. Natural charges in silylene **1a** were calculated as –0.72 on Re and +1.36 on Si, suggesting polarization across this bond, with a calculated Wiberg Bond Index (WBI) of 1.64. These results are consistent with a strong, polarized double bond in silylene **1a**, a bonding motif not previously observed between rhenium and silicon.

In contrast, the Re–Si bond in bridging silane **1b** was modeled by a single σ-bonding interaction (Figure S32).

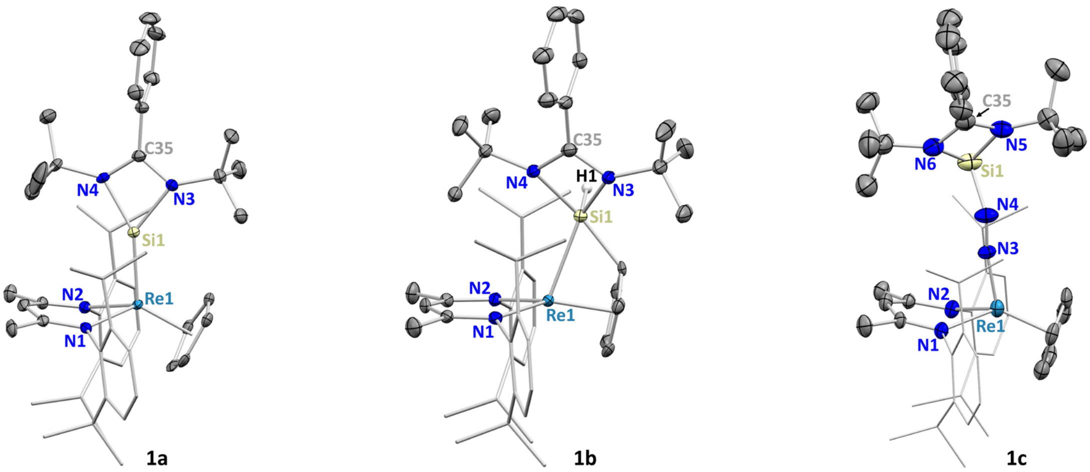

Figure 2. X-ray crystal structures of silylene **1a** (left), bridging silane **1b** (center), and dinitrogen-bridged silylene **1c** (right) shown with 50 % probability ellipsoids. The BDI diisopropylphenyl groups are shown in wireframe, and hydrogen atoms (except for the silane hydrogen in **1b**) are omitted for clarity. Structural metrics are given in Tables S3 and S4.

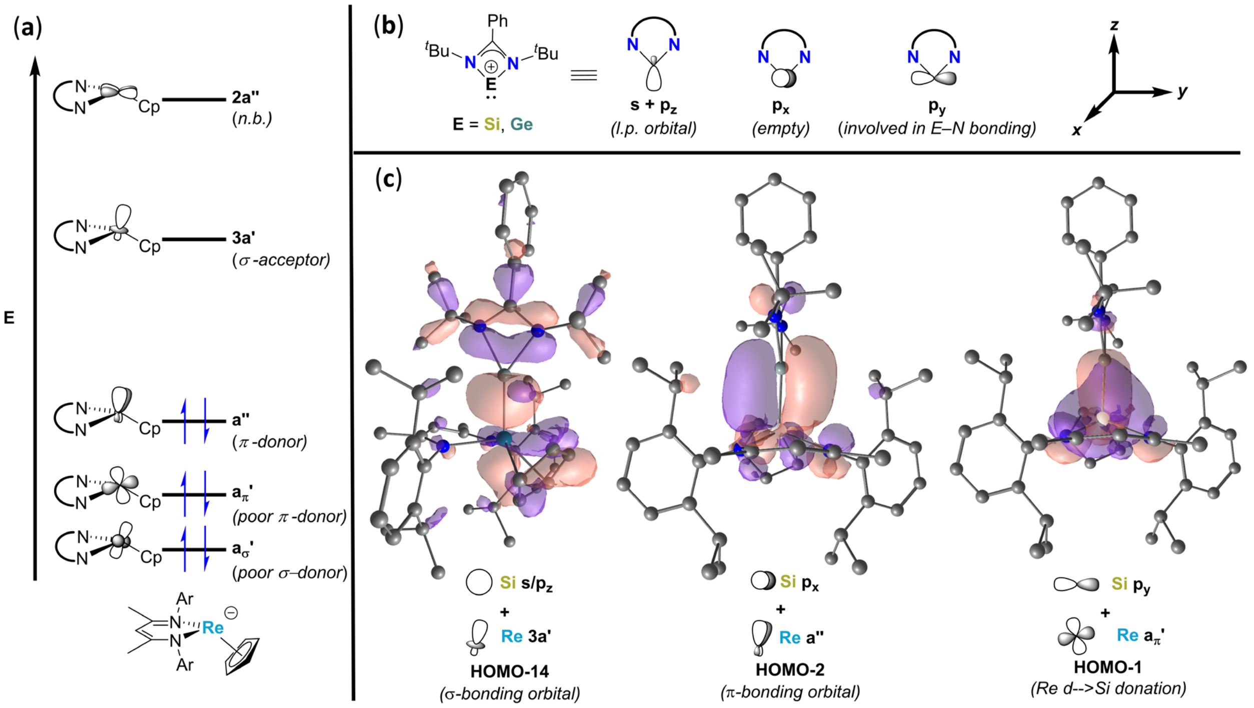

Figure 3. (**a**) Qualitative frontier molecular orbitals of the [Re(η5-Cp)(BDI)]− fragment.[42] (**b**) Qualitative frontier molecular orbitals of a planar E[PhC(N^{t}Bu)$_2$]$^+$ (E = Si, Ge) fragment. (**c**) Renderings of select calculated molecular orbitals of silylene **1a** including a σ-bonding orbital (HOMO–14), π-bonding orbital (HOMO–2), and π-symmetry dative interaction from rhenium towards silicon (HOMO–1).

Corresponding natural charges of –0.72 on Re and +1.48 on Si were found, along with a much smaller WBI of 0.69, relative to that of silylene **1a**. Calculations of dinitrogen-bridged silylene **1c** revealed significant backbonding interactions from rhenium *d*-orbitals into dinitrogen π* orbitals, consistent with the observed redshift of the N–N stretching frequency (Figure S33). In addition, a pure non-bonding lone pair orbital was located on silicon (HOMO–4), as predicted based on the crystal structure.

We next sought to translate the abovementioned reactivity and bonding to the synthesis of heavier tetrylene derivates, especially given that germylene and stannylene derivatives are commonly less reactive than their silicon counterparts and are typically less inclined to be involved in multiple bonding interactions.[11,43] Reaction of Na[Re(η5-Cp)(BDI)] with GeCl[PhC(N^{t}Bu)$_2$] at –78 °C in diethyl ether for one hour led to the formation of a rhenium-germylene, Re(Ge[PhC(N^{t}Bu)$_2$])(η5-Cp)(BDI) (**2**), in 75 % yield (Scheme 2). Solutions of germylene **2** in benzene and toluene were unstable above 0 °C. A variable-temperature NMR study, in which a cold sample of germylene **2** in toluene-d_8 was slowly warmed in the spectrometer from –40 °C to 40 °C, revealed irreversible decomposition of **2** above 0 °C and the appearance of resonances belonging to an unknown byproduct, including a small singlet at –23.59 ppm (Figure S11). For reference, Re–H peaks appear in the –22 to –29 ppm range for closely related complexes reported previously by our group.‡ The unknown resonances may be attributable to formation of a rhenium hydride, possibly due to migration of a hydrogen atom to rhenium from the Cp moiety in concert with substitution of the amidinate-supported germylene at a Cp carbon. However, we were unable to observe any signal attributable to a Re–H stretch in the infrared spectra of a solid sample of germylene **2**.

Neither performing this reaction at ambient temperature nor attempts at thermal conversion of germylene **2** led to an isolable product.

We were also curious as to the importance of amidinate stabilization in tetrylene complexes **1a** and **2** and sought, instead, to form rhenium-tetrylene multiple bonds using readily available divalent tetrylene halide salts. Accordingly, we treated Na[Re(η5-Cp)(BDI)] with $GeCl_2$·dioxane at –78 °C, which led to the isolation of dark purple needles of a germanium-bridged dirhenium complex, Ge[Re(η5-Cp)(BDI)]$_2$ (**3**), in 61 % yield (Scheme 2). Solution NMR spectra of germanium-bridged complex **3** revealed effective C_2 symmetry (see Newman projection in Figure 5b). This observation rules out *syn*- and *anti*-periplanar conformations of **3** in solution at ambient temperature and suggests free rotation about the Re–Ge–Re

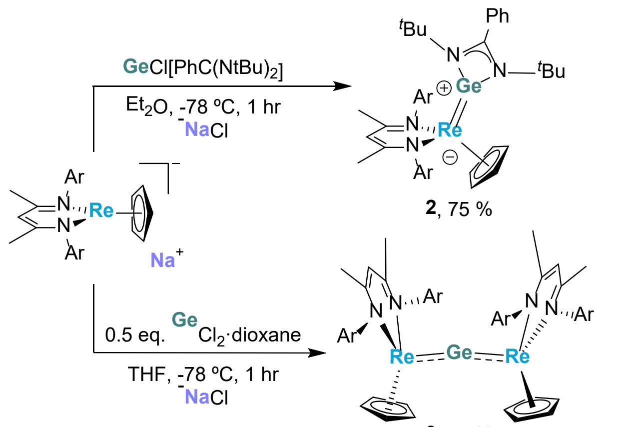

Scheme 2. Syntheses of germylene **2** and germanium-bridged complex **3**. Gradual decomposition of germylene **2** is observed in toluene-d_8 solution above ca. 0 °C to form an unknown rhenium hydride product.

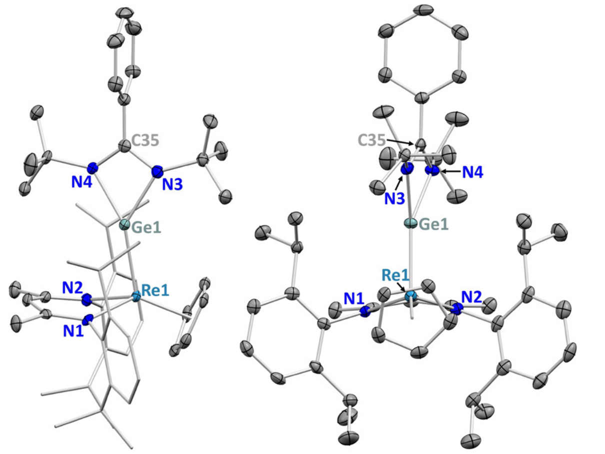

Figure 4. X-ray crystal structure of germylene **2** shown from the side (left) and front (right) with 50% probability ellipsoids. The BDI diisopropylphenyl groups in the side view are shown in wireframe, and hydrogen atoms are omitted for clarity. Structural metrics are given in Table S3.

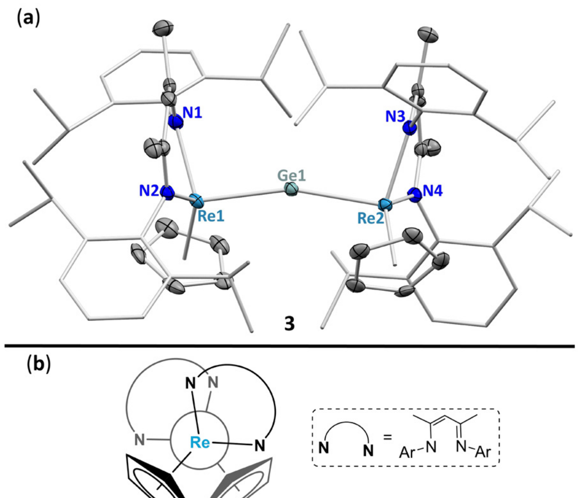

Figure 5. (**a**) X-ray crystal structure of germanium-bridged complex **3** shown with 50 % probability ellipsoids. The BDI diisopropylphenyl groups are shown in wireframe, and hydrogen atoms are omitted for clarity. Structural metrics are given in Table S3. (**b**) Newman projection of **3** viewed along the Re_2–Ge_1–Re_1 axis.

axis is restricted, either by steric restraints or by bonding orbital restrictions.

The solid-state structure of rhenium-germylene **2** closely resembles that of rhenium-silylene **1a**, with a short Re–Ge distance of 2.3322(4) Å and distorted trigonal planar geometry about the germanium atom, as evidenced by Re1–Ge1–N3/N4 angles of 139.76(8) and 151.49(8)° (Figure 4; sum of bond angles about Ge: 356.2°). This geometry is in stark contrast to the iron σ-metallogermylene discussed earlier (Figure 1b), which was synthesized via a similar salt metathesis reaction; in that case, the amidinate-supported germylene was bound in a bent fashion to accommodate a germylene-centered lone pair.[33] In addition, there are several other reported σ-metallogermylenes synthesized from salt metathesis reactions between transition metals (M = Cr, Mo, W) and chlorogermylenes without amidinate stabilization, and they consistently adopt both bent geometries and long M–Ge bond distances.[44–50] The only exception is a case where ligand dissociation at the metal center facilitates metal-germylyne formation, as in the formation of (η^5-Cp)$(CO)_2$Mo≡Ge(C_6H_3-2,6-Mes_2)) (see above, Figure 1a).[26] The short, planar rhenium–germanium bonding arrangement in germylene **2** is indicative of multiple bonding interactions between these atoms, and again suggests the absence of a localized non-bonding lone pair on germanium. For reference, the few structurally reported Re–Ge single bonds range from 2.5446(3)–2.6383(4) Å,[27,51,52] while Gladysz and coworkers found a slightly shorter Re–Ge distance of 2.4738(6) Å due to the ionicity of a triflate group on germanium, which in effect led to double bond character of the rhenium–germanium bond.[53] Additional comparative insight into the rhenium-germanium bond distances of both germylene **2** and germanium-bridged complex **3** can be made with the rhenium germylene (Re=GeR_2: 2.3253(4)–2.3422(4) Å) and germylyne (Re≡GeR: 2.2609(3)–2.2772(2) Å) complexes synthesized by Filippou and coworkers (Figure 1a).[29]

Germanium-bridged complex **3** adopts a gauche conformation in the solid state (dihedral angle of 71.3° between the Cp centroids), consistent with its solution state C_2 symmetry

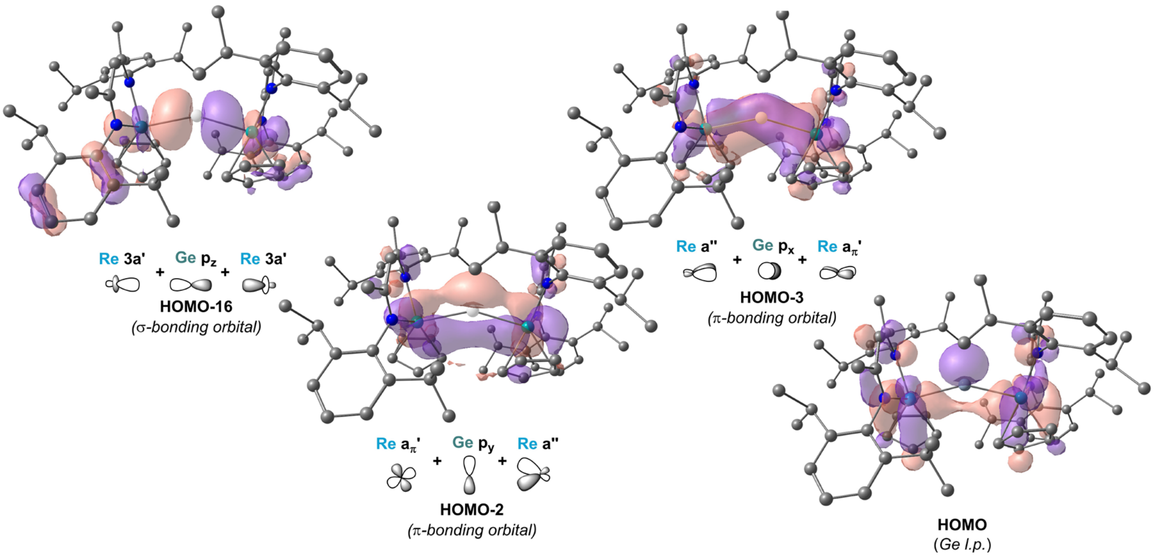

Figure 6. Renderings of select calculated molecular orbitals of **3** as a singlet, along with qualitative relevant fragment orbitals shown below certain renderings.

(Figure 5a). Additionally, the Re–Ge distances were measured at 2.4395(5) Å and 2.4367(5) Å, with a slightly bent Re1–Ge1–Re2 angle of 163.18(2)°. This represents a rare example of μ_2-tetrelido coordination involving a heavy group 14 atom bridged between two transition metal centers, with the most prevalent analogous system based on a structurally similar [Mn(η^5-C_5R_5)(CO)$_2$] fragment bridged by germanium, tin, and lead.[54–60] More recently, however, the first bridging silicon centers have also been reported within different transition metal systems.[61,62]

We also investigated the electronic structures of germylene **2** and germanium-bridged complex **3** computationally. Natural bond orbital analysis of rhenium-germylene **2** revealed a nearly identical bonding scheme to rhenium-silylene **1a**. Two covalent bonding interactions were identified, with a σ-symmetry orbital containing slightly more germanium character than the analogous silicon contribution in **1a** and a π-type orbital with more rhenium character (Table S5). Again, second-order perturbation analysis suggests a 76.5 kcal/mol donation from the filled a_π' orbital on rhenium to germanium (Figure S34). The natural charges for complex **2** were found to be –0.67 on Re and 1.32 on Ge, with a WBI of 1.50. Given the orbital analysis discussed previously for silylene **1a**, a reasonable description of the bonding in germylene **2** is as a polarized double bond between rhenium and germanium.

Natural bond orbital analysis of the singlet structure of germanium-bridged **3** revealed WBI's for the Re–Ge bonds of 1.08 and 1.10 (larger than in silane **1b** and σ-metallostannylene **4** (see below) but lower than in silylene **1a** and germylene **2**), consistent with partial multiple bonding between these atoms. NBO calculations identified σ-type bonds between each Re–Ge internuclear axis that consist of a *p*-based germanium orbital with rhenium-based orbitals (Figure 6, HOMO-16). In addition, inspection of the Kohn-Sham molecular orbitals reveal geometrically orthogonal orbitals of π-symmetry (HOMO-3 and HOMO-2), suggesting some degree of delocalized π-bonding about the Re–Ge–Re axis. The HOMO orbital, however, represents a germanium-centered lone pair that is not wholly involved in bonding with rhenium, and may be responsible for the slight bending of the Re1–Ge–Re2 angle.

The optimized geometry of germanium-bridged complex **3**, calculated as a singlet, deviated slightly from that of the experimentally determined structure (see Table S6 for full comparison of experimental versus computational geometries and electronic energies of **3**). Surprisingly, we found that calculating the optimized geometry of **3** as a triplet led to a slightly more agreeable structure and a quintet calculation led to the most accurate geometry. However, we have no reason to believe **3** has a paramagnetic ground state, as an Evans method measurement[63,64] of **3** in C_6D_6 showed no evidence of a magnetic moment and the NMR spectrum showed well resolved, narrow linewidth signals with chemical shifts in line with other diamagnetic complexes containing this [Re(η^5-Cp)(BDI)] fragment).

Interestingly, a previous molecular orbital computational study looked into the relevant bonding orbitals of μ_2-Ge[Mn(η^5-C_5R_5)(CO)$_2$]$_2$.[65] Solid-state structures of μ_2-Ge[Mn(η^5-C_5R_5)(CO)$_2$]$_2$ adopted *anti*-periplanar and gauche conformations (MeC_5H_4 or C_5H_5 = *anti*-periplanar, C_5Me_5 = gauche) with Mn–Ge–Mn angles of 180±3°. However, solution IR and NMR measurements revealed facile rotation about the Mn=Ge=Mn axis. Experimental and computational data led the authors to argue that there was not "allene-like" bonding in μ_2-Ge[Mn(η^5-Cp)(CO)$_2$]$_2$, as orbital restrictions in an allene-type molecule would prevent free rotation about the central axis. Instead, they described the Mn=Ge=Mn bonding fragment as containing "partial triple bonding" between each manganese and germanium atom, leading to a nearly cylindrically symmetric π-system in which free rotation about the Mn–Ge–Mn axis is orbitally allowed.

Given the similarities to germanium-bridged dirhenium complex **3**, it is curious that free rotation about the Re–Ge–Re bond axis in solution is not observed. However, this may be a result of germanium retaining some *s*-based lone pair character (HOMO), leading to slight bending of the Re–Ge–Re axis, which may be a result of germanium-bridged complex **3** containing two fewer valence electrons relative to μ_2-Ge[Mn(η^5-C_5R_5)(CO)$_2$]$_2$ (due to the difference between anionic BDI versus neutral CO ligands). The slightly bent geometry precludes a cylindrically symmetric π-system; thus, rotation about the Re–Ge–Re axis is orbitally non-degenerate and leads to an energetic barrier that prevents facile rotation about the Re–Ge–Re axis. It is also possible, however, that the barrier to rotation is sterically determined. For example, another bridged dirhenium complex reported by our group, [ZnRe(η^5-Cp)(BDI)]$_2$, also did not freely rotate in solution about the Re–Zn–Zn–Re axis.[35] The lack of rotation in this example was almost certainly due to steric constraints, as the compound was devoid of any Re–Zn π-bonding, and as such we cannot rule out similar steric factors in **3**.

Continuing to descend the group 14 column, we found that reactions between Na[Re(η^5-Cp)(BDI)] and both $SnCl_2$ and $PbCl_2$ were unsuccessful in producing any isolable Re–E (E = Sn, Pb) bonded products. Instead, we noted the formation of Re(η^5-Cp)(BDI), a common byproduct in reactions with this rhenium(I) starting material upon one-electron oxidation, suggesting that, in contrast to $GeCl_2$, both $SnCl_2$ and $PbCl_2$ are reduced by Na[Re(η^5-Cp)(BDI)]. However, use of an amidinate-supported stannylene led to the desired reactivity. Addition of Na[Re(η^5-Cp)(BDI)] to SnCl[PhC(N^{t}Bu)$_2$] in Et_2O at –78 °C led to a dark purple solution. Following a cold workup and crystallization from pentane at ambient temperature for two hours, we obtained the σ-metallostannylene, Re(Sn[PhC(N^{t}Bu)$_2$])(η^5-Cp)(BDI) (**4**), in 77 % yield (Scheme 3). Longer crystallization times or slower reaction workups with ambient temperature

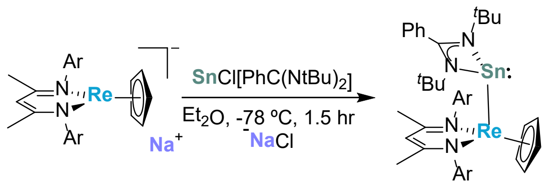

4, 77 %

Scheme 3. Synthesis of σ-metallostannylene **4**. Gradual decomposition of **4** is observed in toluene-d_8 solution above ca. 0 °C to form Re(η^5-Cp)(BDI)[35] and an unknown amidinate product.

solvents led to substantial degradation. This decomposition was observed in a variable temperature ^{1}H NMR experiment in which a fresh sample of σ-metallostannylene **4** was prepared in cold toluene-d_8 and slowly allowed to warm from –63 °C to 37 °C in the spectrometer (Figures S16-S18). Initial spectra at –63 °C show that the two amidinate *tert*-butyl groups are distinguishable as separate singlets, suggesting restricted rotation about the Re–Sn bond. However, these singlets coalesce around –3 °C, as the relatively small energetic barrier to rotation is overcome. Around this same temperature, however, signals attributable to decomposition products appear, and upon warming to 17 °C, resonances for both Re(η^5-Cp)(BDI) and an unknown amidinate byproduct are observed. Unfortunately, attempts to observe a ^{119}Sn{^{1}H} resonance for σ-metallostannylene **4** were unsuccessful.

Contrary to the planar tetrylene geometries observed for silylene **1a** and germylene **2**, σ-metallostannylene **4** adopts a bent coordination geometry at the tin center in the solid state (Figure 7). In this case, the Re–Sn bond distances for the two molecules of σ-metallostannylene **4** in the asymmetric unit were found to be 2.7532(5) and 2.7562(5) Å, which are more than 0.4 Å longer than that of the Re–Ge bond in germylene **2**. This is a significant lengthening of the bond, and the Re–Sn distance in σ-metallostannylene **4** falls in line with reported Re–Sn single bonds, with the additional feature that this is the first example of rhenium bound to a formally Sn(II) center. The Re–Sn–N3/N4 angles range from 124.35(9)° to 129.58(9)°, indicating significant deviation from the planarity observed in silylene **1a** and germylene **2**, likely due to the accommodation of a tin-based lone pair. While the bent geometry in **4** is slightly more planar relative to the few previously reported σ-metallostannylene complexes,[45,46,50,66–71] the geometry is generally more consistent with a σ-metallotetrylene structure than with rhenium-silylene and -germylene complexes **1a** and **2**.

Computational investigations of σ-metallostannylene **4** corroborated the presence of a Re–Sn single bond with a non-bonding lone pair orbital on tin (Figure 8). The natural bonding

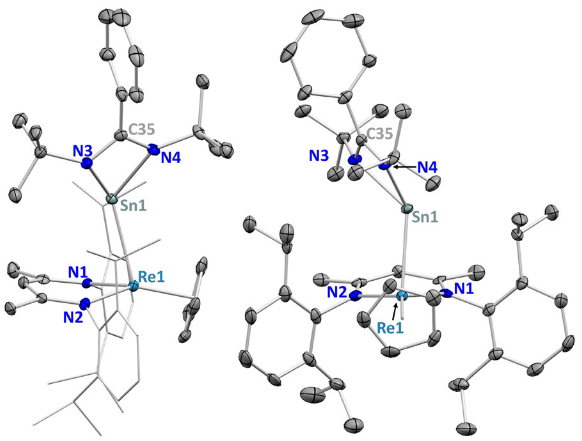

Figure 7. X-ray crystal structure of σ-metallostannylene **4** shown from the side (left) and front (right) with 50% probability ellipsoids. The BDI diisopropylphenyl groups in the side view are shown in wireframe, and hydrogen atoms are omitted for clarity. A molecule of pentane, as well as the second molecule of **4** in the asymmetric unit, are also omitted. Structural metrics are given in Table S3.

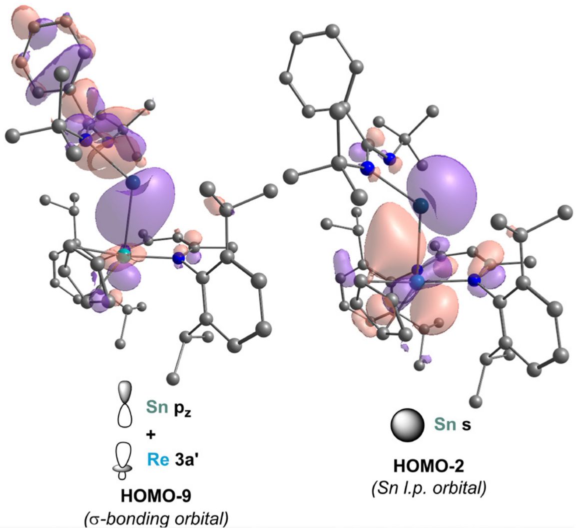

Figure 8. Renderings of select calculated molecular orbitals of **4** including a σ-bonding orbital (HOMO–9) and tin lone pair orbital (HOMO-2), along with qualitative relevant fragment orbitals shown below each rendering.

orbital of **4** exhibits σ-symmetry and is polarized towards rhenium, with a WBI of 0.9 and natural charges of –0.43 on Re and 1.18 on Sn. The lone pair of tin in **4** therefore does not interact significantly with rhenium-based orbitals, as is the case in silylene **1a** and germylene **2**, leading to the observed σ-metallostannylene structure in **4**. It may be the case that the more diffuse orbitals of tin and decreased mixing of its *s* and *p* atomic orbitals, relative to silicon and germanium, leads to less favorable orbital overlap with rhenium *d*-orbitals and precludes the necessary orbital mixing required for the trigonal planar bonding geometry seen in silylene **1a** and germylene **2**. This type of geometric distortion upon moving to a heavier group 14 analogue is consistent with trends seen previously between heavy main group elements.[11]

Conclusions

We have demonstrated that salt metathesis reactions between a series of amidinate-supported tetrylenes, ECl[PhC(N^{t}Bu)$_2$] (E = Si, Ge, Sn), and the sodium salt of a bulky rhenium(I) cyclopentadienide β-diketiminate leads to rhenium metallotetrylenes with unusual bonding arrangements. While the silicon and germanium analogues engage in short, polarized multiple bonds with rhenium through incorporation of the tetrylene-based lone pair in bonding along with backdonation from rhenium *d*-orbitals to tetrylene *p*-orbitals, the heavier stannylene compound retains its non-bonding lone pair orbital in a bent geometry, consistent with established disparities in the bonding of heavier main group elements. In addition, we found that manipulation of reaction conditions, especially temperature, leads to multiple products in the case of reactions with SiCl[PhC(N^{t}Bu)$_2$]. We isolated a complex with a very unusual silane bridge between rhenium and a Cp ligand and observed a diazene-functionalized silylene via dinitrogen activation. Finally, we accessed a rare example of a μ$_2$-tetrelido complex featuring a naked germanium atom bridged between two rhenium centers that had a slightly bent geometry relative to those of related complexes. Investigations into potential reactivity across this array of polarized M–E bonds is ongoing and will be the subject of future reports.

Conflicts of interest

There are no conflicts to declare.

Acknowledgements

This research was funded by the NSF (Grant No. CHE-1465188 and 1954612 to J.A. and R.G.B.). We thank Dr. Hasan Celik and UC Berkeley's NMR facility in the College of Chemistry (CoC-NMR) for spectroscopic assistance. Instruments in the CoC-NMR are supported in part by NIH S10OD024998. The Advanced Light Source (ALS) is supported by the Director, Office of Science, Office of Basic Energy Sciences, of the U.S. DOE under Contract No. DE-AC02-05CH11231. Dr. Simon J. Teat is thanked for his assistance during crystallography experiments at the ALS. We also acknowledge Dr. Nick Settineri and UC Berkeley's CheXray facility for crystallographic assistance. Jade I. Fostvedt and Dr. Michael A. Boreen are thanked for helpful discussions. Prof. Simon Humphrey (University of Texas, Austin) is thanked for a generous donation of rhenium. L. M. is a senior member of the Institut Universitaire de France. CalMip is acknowledged for a generous grant of computing time.

Notes and references

‡ Re(H)(η^5-Cp)(BDI),[35] Re(H)(η^5-$C_5H_4SiMe_3$)(BDI),[34] FB[(η^5-C_5H_4)Re(H)(BDI)]$_2$.[72]

1 Y. P. Zhou and M. Driess, *Angew. Chemie - Int. Ed.*, 2019, **58**, 3715–3728.
2 J. W. Herndon, *Coord. Chem. Rev.*, 2019, **401**, 213051.
3 H. Fischer, P. Hofmann, F. R. Kreissl, R. R. Schrock, U. Schubert and K. Weiss, *Carbyne Complexes.*, VCH, Weinheim, 1988.
4 U. Schubert, *Coord. Chem. Rev.*, 1984, **55**, 261–286.
5 E. O. Fischer, *Adv. Organomet. Chem.*, 1976, **14**, 1–32.
6 W. A. Nugent, *Metal-ligand multiple bonds : the chemistry of transition metal complexes containing oxo, nitrido, imido, alkylidene, or alkylidyne ligands*, Wiley, New York, 1988.
7 W. D. Wulff, in *Comprehensive Organic Synthesis*, Elsevier, 1991, pp. 1065–1113.
8 S. B. T. Nguyen, L. K. Johnson, R. H. Grubbs and J. W. Ziller, *J. Am. Chem. Soc.*, 1992, **114**, 3974–3975.
9 O. M. Ogba, N. C. Warner, D. J. O'Leary and R. H. Grubbs, *Chem. Soc. Rev.*, 2018, **47**, 4510–4544.
10 M. Okazaki, H. Tobita and H. Ogino, *J. Chem. Soc. Dalt. Trans.*, 2003, **3**, 493–506.
11 P. P. Power, *Nature*, 2010, **463**, 171–177.
12 W. Petz, *Chem. Rev.*, 1986, **86**, 1019–1047.
13 K. Junold, J. A. Baus, C. Burschka, T. Vent-Schmidt, S. Riedel and R. Tacke, *Inorg. Chem.*, 2013, **52**, 11593–11599.
14 C. Shan, S. Yao and M. Driess, *Chem. Soc. Rev.*, 2020, **49**, 6733–6754.
15 M. Asay, C. Jones and M. Driess, *Chem. Rev.*, 2011, **111**, 354–396.
16 R. Waterman, P. G. Hayes and T. D. Tilley, *Acc. Chem. Res.*, 2007, **40**, 712–719.
17 B. Blom, M. Stoelzel and M. Driess, *Chem. - A Eur. J.*, 2013, **19**, 40–62.
18 J. Baumgartner and C. Marschner, *Rev. Inorg. Chem.*, 2014, **34**, 119–152.
19 L. Álvarez-Rodríguez, J. A. Cabeza, P. García-Álvarez and D. Polo, *Coord. Chem. Rev.*, 2015, **300**, 1–28.
20 J. A. Cabeza, P. García-Álvarez and D. Polo, *Eur. J. Inorg. Chem.*, 2016, **2016**, 10–22.
21 J. Y. Corey, *Chem. Rev.*, 2016, **116**, 11291–11435.
22 R. Tacke and T. Ribbeck, *Dalt. Trans.*, 2017, **46**, 13628–13659.
23 M. C. Lipke, A. L. Liberman-Martin and T. D. Tilley, *Angew. Chemie - Int. Ed.*, 2017, **56**, 2260–2294.
24 H. Hashimoto and H. Tobita, *Coord. Chem. Rev.*, 2018, **355**, 362–379.
25 P. G. Hayes, Z. Xu, C. Beddie, J. M. Keith, M. B. Hall and T. D. Tilley, *J. Am. Chem. Soc.*, 2013, **135**, 11780–11783.
26 R. S. Simons and P. P. Power, *J. Am. Chem. Soc.*, 1996, **118**, 11966–11967.
27 K. V. Zaitsev, E. A. Kuchuk, A. V. Churakov, M. A. Navasardyan, M. P. Egorov, G. S. Zaitseva and S. S. Karlov, *Inorganica Chim. Acta*, 2017, **461**, 213–220.
28 G. Balázs, L. J. Gregoriades and M. Scheer, *Organometallics*, 2007, **26**, 3058–3075.
29 A. C. Filippou, U. Chakraborty and G. Schnakenburg, *Chem. - A Eur. J.*, 2013, **19**, 5676–5686.
30 C. W. So, H. W. Roesky, J. Magull and R. B. Oswald, *Angew. Chemie - Int. Ed.*, 2006, **45**, 3948–3950.
31 S. Nagendran, S. S. Sen, H. W. Roesky, D. Koley, H. Grubmüller, A. Pal and R. Herbst-Irmer, *Organometallics*, 2008, **27**, 5459–5463.
32 S. S. Sen, M. P. Kritzler-Kosch, S. Nagendran, H. W. Roesky, T. Beck, A. Pal and R. Herbst-Irmer, *Eur. J. Inorg. Chem.*, 2010, **2010**, 5304–5311.
33 C. Jones, R. P. Rose and A. Stasch, *Dalt. Trans.*, 2008, 2871.
34 T. D. Lohrey, R. G. Bergman and J. Arnold, *Dalt. Trans.*, 2019, **48**, 17936–17944.
35 T. D. Lohrey, L. Maron, R. G. Bergman and J. Arnold, *J. Am. Chem. Soc.*, 2019, **141**, 800–804.
36 F. Uhlig, in *Organosilicon Compounds: Experiment (Physico-Chemical Studies) and Applications*, Elsevier, 2017, pp. 59–77.
37 K. K. Irikura, *J. Phys. Chem. Ref. Data*, 2007, **36**, 389–397.
38 T. D. Lohrey, J. I. Fostvedt, R. G. Bergman and J. Arnold, *Chem. Commun.*, 2020, **56**, 3761–3764.
39 B. Dudle, K. Rajesh, O. Blacque and H. Berke, *Organometallics*, 2011, **30**, 2986–2992.
40 I. Manners, *Adv. Mater.*, 1994, **6**, 68–71.
41 K. P. Huber and G. Herzberg, *Molecular Spectra and Molecular Structure*, Springer US, 1979.
42 B. E. R. Schilling, R. Hoffmann and D. L. Lichtenberger, *J. Am. Chem. Soc.*, 1979, **101**, 585–591.

43 S. Nagendran and H. W. Roesky, *Organometallics*, 2008, **27**, 457–492.

44 K. K. Pandey and C. Jones, *Organometallics*, 2013, **32**, 3395–3403.

45 H. Lei, J. D. Guo, J. C. Fettinger, S. Nagase and P. P. Power, *Organometallics*, 2011, **30**, 6316–6322.

46 S. Inoue and M. Driess, *Organometallics*, 2009, **28**, 5032–5035.

47 P. Jutzi and C. Leue, *Organometallics*, 1994, **13**, 2898–2899.

48 L. Pu, B. Twamley, S. T. Haubrich, M. M. Olmstead, B. V. Mork, R. S. Simons and P. P. Power, *J. Am. Chem. Soc.*, 2000, **122**, 650–656.

49 K. Inomata, T. Watanabe and H. Tobita, *J. Am. Chem. Soc.*, 2014, **136**, 14341–14344.

50 Y. N. Lebedev, U. Das, G. Schnakenburg and A. C. Filippou, *Organometallics*, 2017, **36**, 1530–1540.

51 R. D. Adams, B. Captain, C. B. Hollandsworth, M. Johansson and J. L. Smith, *Organometallics*, 2006, **25**, 3848–3855.

52 G. Albertin, S. Antoniutti and J. Castro, *J. Organomet. Chem.*, 2012, **696**, 4191–4201.

53 K. E. Lee, A. M. Arif and J. A. Gladysz, *Organometallics*, 1991, **10**, 751–760.

54 W. Gäde and E. Weiss, *J. Organomet. Chem.*, 1981, **213**, 451–460.

55 D. Melzer and E. Weiss, *J. Organomet. Chem.*, 1984, **263**, 67–73.

56 W. A. Herrmann, H. -J Kneuper and E. Herdtweck, *Angew. Chemie Int. Ed. English*, 1985, **24**, 1062–1063.

57 W. A. Herrmann, H. -J Kneuper and E. Herdtweck, *Chem. Ber.*, 1989, **122**, 437–444.

58 F. Ettel, G. Huttner and W. Imhof, *J. Organomet. Chem.*, 1990, **397**, 299–307.

59 F. Ettel, G. Huttner and L. Zsolnai, *Angew. Chemie Int. Ed. English*, 1989, **28**, 1496–1498.

60 J. D. Korp, I. Bernal, R. Hörlein, R. Serrano and W. A. Herrmann, *Chem. Ber.*, 1985, **118**, 340–347.

61 R. C. Handford, P. W. Smith and T. D. Tilley, *J. Am. Chem. Soc.*, 2019, **141**, 8769–8772.

62 P. Ghana, M. I. Arz, U. Chakraborty, G. Schnakenburg and A. C. Filippou, *J. Am. Chem. Soc.*, 2018, **140**, 7187–7198.

63 D. F. Evans, *J. Chem. Soc.*, 1959, **81**, 2003–2005.

64 G. A. Bain and J. F. Berry, *J. Chem. Educ.*, 2008, **85**, 532–536.

65 N. M. Kostić and R. F. Fenske, *J. Organomet. Chem.*, 1982, **233**, 337–351.

66 B. E. Eichler, A. D. Phillips, S. T. Haubrich, B. V. Mork and P. P. Power, *Organometallics*, 2002, **21**, 5622–5627.

67 P. G. Hayes, C. W. Gribble, R. Waterman and T. D. Tilley, *J. Am. Chem. Soc.*, 2009, **131**, 4606–4607.

68 J. D. Queen, A. C. Phung, C. A. Caputo, J. C. Fettinger and P. P. Power, *J. Am. Chem. Soc.*, 2020, **142**, 2233–2237.

69 P. W. Smith, R. C. Handford and T. Don Tilley, *Organometallics*, 2019, **38**, 4060–4065.

70 M. A. Stewart, T. B. Ditri, L. A. Labios, A. L. Rheingold and J. S. Figueroa, *Chem. Commun.*, 2011, **47**, 406–408.

71 H. J. Liu, J. Guihaumé, T. Davin, C. Raynaud, O. Eisenstein and T. D. Tilley, *J. Am. Chem. Soc.*, 2014, **136**, 13991–13994.

72 T. D. Lohrey, G. Rao, D. W. Small, E. T. Ouellette, R. G. Bergman, R. D. Britt and J. Arnold, *J. Am. Chem. Soc.*, 2020, **142**, 13805–13813.

Please do not adjust margins